

# Comparative Analysis of State and Parameter Estimation Techniques for Power System Frequency Dynamics

Bidur Poudel<sup>†</sup>, Pooja Aslami, Tara Aryal, Niranjan Bhujel, Astha Rai, Manisha Rauniyar, Hossein Moradi Rekabdarkolaei, Ujjwol Tamrakar, Timothy M. Hansen, and Reinaldo Tonkoski

**Abstract**—Dynamic state and parameter estimation in current and future power systems are critical for advanced monitoring, control, and protection. There are numerous methods to perform dynamic state and parameter estimation; this paper compares the accuracy and computational time of four methods (i.e., Kalman filter (KF), extended Kalman filter (EKF), unscented Kalman filter (UKF), and moving horizon estimation (MHE)) designed to estimate the states and parameters for frequency dynamics of a power system. A simulation study was conducted using Matlab/Simulink by introducing Gaussian and non-Gaussian noise in the measurements. Results under Gaussian noise showed similar accuracy performance for all filters. EKF and UKF presented convergence or numerical instability issues due to incorrect initial guesses of parameters. MHE did not present convergence issues, however, required comparatively higher computation time. Nonetheless, the MHE could still be implemented in real-time for state and parameter estimation of power system. The impact of non-Gaussian noise on the methods was inconclusive and will require further study.

**Index Terms**—Computational tractability, extended Kalman filter, Kalman filter, moving horizon estimation, state and parameter estimation, unscented Kalman filter.

## I. INTRODUCTION

With a significant increase in distributed energy resources (DER) in power systems and advanced control structures, the grid is becoming more dynamic. Thus, to adaptively adjust the control and operation of such power systems, methods

This work is supported by the U.S. Department of Energy Office of Science, Office of Electricity Microgrid R&D Program, and Office of Energy Efficiency and Renewable Energy Solar Energy Technology Office under the EPSCoR grant number DE-SC0020281. This work made use of the Opal-RT real-time simulator purchased as part of the National Science Foundation (NSF) grant number MRI-1726964.

The work at Sandia (Ujjwol Tamrakar) is supported by the US Department of Energy, Office of Electricity, Energy Storage Program.

B. Poudel, P. Aslami, T. Aryal, N. Bhujel, A. Rai, M. Rauniyar, H. M. Rekabdarkolaei, T. M. Hansen, and R. Tonkoski are with the Department of Electrical Engineering and Computer Science, South Dakota State University, Brookings, South Dakota, 57007 USA, (<sup>†</sup>corresponding email: Bidur.Poudel@jacks.sdstate.edu).

U. Tamrakar is with the Sandia National Laboratories, Albuquerque, New Mexico, USA.

Sandia National Laboratories is a multi-mission laboratory managed and operated by National Technology and Engineering Solutions of Sandia, LLC., a wholly owned subsidiary of Honeywell International, Inc., for the U.S. Department of Energy National Nuclear Security Administration under contract DE-NA-0003525. This paper describes objective technical results and analysis. Any subjective views or opinions that might be expressed in the paper do not necessarily represent the views of the U.S. Department of Energy or the United States Government.

that accurately measure the time-varying power system states and parameters are required. Due to the lack of accurate and computationally efficient models, the increasing availability of fast-sampled, time-synchronized measurements, and the advances in the capability, scalability, and affordability of computing and communications, dynamic state and parameter estimation is becoming increasingly critical for enabling advanced monitoring, control, and protection of electric power grids [1].

Fast frequency support (i.e., frequency support acting before primary frequency response) is a critical service to the grid that requires accurate and timely measurements. Energy storage systems (ESS) or other DERs can be used to provide fast frequency support. However, it requires dynamic state estimators due to the characteristics of frequency measurements required for the controller implementation. Moreover, during estimation, the system can be perturbed using an excitation signal, which is generated from ESS and whose suitability depends on the topology of ESS. Sensor data can be noisy, and low-pass filters can introduce relatively large delays in the measurement leading to degradation of the control and monitoring process that can lead to instability [2]. In addition to states, parameters of the system may also need to be estimated for implementing predictive control architectures. Because of changes in operating points, configurations, aging, etc., system parameters can change frequently over time and need to be monitored (e.g., system inertia constant changes based on dispatch of generation).

Several filters have been proposed for state and parameter estimation, including the least square estimator (LSE), weighted least square estimator (WLSE), Kalman filter (KF), extended Kalman filter (EKF), unscented Kalman filter (UKF), particle filter (PF), moving horizon estimation (MHE), etc. In [3], the strengths and limitations of these filters, except MHE, along with their applications, have been discussed. However, the given strengths and limitations were based on literature without implementing filters in any system. An MHE approach was proposed in [2] for the estimation of change in frequency, rate-of-change-of-frequency (ROCOF), inertia constant, and damping constant to provide fast frequency dynamic support for a microgrid benchmark. Performance comparison of EKF, UKF, PF, and enhanced unscented Kalman filter (E-UKF) based on accuracy, efficiency, and speed was carried out

in [4], [5]. The paper, however, focused on the estimation of system states and did not include parameter estimation.

The implementation of filters varies depending on the application domain, timescale requirements, and system complexity. For fast frequency support, accurate filters that provide fast estimates are required. This paper first summarizes the design criteria, then evaluates the characteristics, accuracy, and computation time requirement of KF, EKF, UKF, and MHE for both state and parameter estimation for the frequency dynamics of a microgrid.

The paper is organized as follows: Section II explains the filtering algorithms and design criteria. The frequency dynamics model, simulation setup, and parameter selection for implementing the filters are described in Section III. In Section IV, different filters are compared based on computation time and accuracy using different error metrics. Finally, the conclusions are presented in Section V.

## II. STATE AND PARAMETER ESTIMATION TECHNIQUES AND THEIR DESIGN CRITERIA

Due to the underlying application domain of power system frequency dynamics, this paper focuses on dynamic filters for state and parameter estimation in the presence of noisy measurements. To implement the estimators for a given dynamic system, different design criteria need to be carefully addressed. This section will first explain common design criteria among all estimators, and then discuss individual criteria of four dynamic filters: KF, EKF, UKF, and MHE.

### A. Common Design Criteria of Filters

The common design criteria of the four estimators (filters) presented in this paper are the sampling time ( $T_s$ ), and the process and measurement noise ( $\mathbf{w}_k$  and  $\mathbf{v}_k$ , respectively). The sampling time (discrete rate of data measurement) should be selected based on the time constants of the system dynamics. The time constants can be calculated as the eigenvalues of the state matrix,  $\mathbf{A}$ , and  $T_s$  should be chosen to be 10–20× smaller than the system time constant [6].

Each of the filters uses a prediction model and measurements to infer the system state, both have a corresponding noise. Let  $n_x$  and  $n_y$  be the number of states and measurements, respectively. Process noise ( $\mathbf{w}_k \in \mathbb{R}^{n_x}$ ) is the error between the actual system and prediction model used in the estimator, and measurement noise ( $\mathbf{v}_k \in \mathbb{R}^{n_y}$ ) is the error between the true value and measured data. The filters *weight* their impact on the estimate based on the covariance of the noise. For a system with  $n_x$  states and  $n_y$  measurements, let  $\mathbf{Q} \in \mathbb{R}^{n_x \times n_x}$  and  $\mathbf{R} \in \mathbb{R}^{n_y \times n_y}$  be the covariance matrices of process and measurement noise, respectively. In this paper, the noise distributions are assumed to be known, hence  $\mathbf{Q}$  and  $\mathbf{R}$  are directly calculable. If these are unknown/unable to be characterized, an autocovariance least-square approach can be used to determine  $\mathbf{Q}$  and  $\mathbf{R}$  [7].

Additionally, observability analysis should be performed to provide guidelines for measurement selection [8] and to determine if there is a solution to the estimation problem.

Each of the filters in this paper will use an excitation signal to perturb the system, which has a significant impact on filter performance, but the design of these signals is not considered in this work. For a discussion on the design of excitation signals, the reader is directed towards [9].

### B. Kalman Filter Design

The KF family (KF, UKF, EKF in this paper) of state estimators are proven optimal assuming Gaussian noise characteristics; depending on the noise distribution, they may fail if the noise is non-Gaussian. Other than design parameters mentioned in the previous section, KF-type estimators also require an initial guess of states and covariance. The closer the initial guess to the true value, the faster KF converges and vice-versa. After the estimator initially converges, the error in the initial guess has no impact on estimation afterward. If a poor initial guess is taken, the filters may diverge; domain knowledge can be used to specify the initial guess (e.g., flat start in power flow).

In KF-type estimators, model parameters to be estimated are also treated as states, the dynamics of which are constant, and are simultaneously estimated with the states [10]. In general, when parameters are also considered, the estimation problem becomes non-linear and the traditional KF is no longer applicable. For the UKF and EKF, a parameter noise term is added (process noise for parameters as a state) to account for variation in the parameters [10].

1) *Kalman Filter*: KF, also called linear quadratic estimating filter, is only applicable for linear systems. It is shown to be optimal if the noise is Gaussian noise, but it can only estimate the system state. Consider the discretized linear system and measurement model with  $n_u$  inputs as below [11]:

$$\mathbf{x}_k = \mathbf{A}_d \mathbf{x}_{k-1} + \mathbf{B}_d \mathbf{u}_{k-1} + \mathbf{w}_{k-1} \quad (1)$$

$$\mathbf{y}_k = \mathbf{C}_d \mathbf{x}_k + \mathbf{v}_k \quad (2)$$

where at discrete time instant  $k$ ,  $\mathbf{x}_k \in \mathbb{R}^{n_x}$  is the system state,  $\mathbf{u}_k \in \mathbb{R}^{n_u}$  is the input,  $\mathbf{y}_k \in \mathbb{R}^{n_y}$  is the measurement, and  $\mathbf{A}_d \in \mathbb{R}^{n_x \times n_x}$ ,  $\mathbf{B}_d \in \mathbb{R}^{n_x \times n_u}$ , and  $\mathbf{C}_d \in \mathbb{R}^{n_y \times n_x}$  are the discretized state, input, and measurement matrices, respectively.

The KF operates recursively, i.e., it combines estimates from the previous discrete-time with a prediction model and current discrete-time measurement to provide the estimate at the current discrete-time. The process consists of two steps: the prediction step and the update step. In the prediction step, the states and their respective covariance (which are estimated at the previous discrete time instant) are passed through the state equation to compute the prior states and their covariance [12]. This occurs in the following two equations:

$$\hat{\mathbf{x}}_k^- = \mathbf{A}_d \hat{\mathbf{x}}_{k-1} + \mathbf{B}_d \mathbf{u}_{k-1} \quad (3)$$

$$\hat{\mathbf{P}}_k^- = \mathbf{A}_d \hat{\mathbf{P}}_{k-1} \mathbf{A}_d^\top + \mathbf{Q} \quad (4)$$

where at discrete time instant  $k$  (and  $k-1$  indicates the previous timestep/estimate),  $\hat{\mathbf{x}}_{k-1}$  and  $\hat{\mathbf{P}}_{k-1}$  represent the previous estimated states and their covariance matrices, respectively,

and  $\hat{\mathbf{x}}_k^-$  and  $\hat{\mathbf{P}}_k^-$  are the prior estimate of states and their covariance matrices, respectively.

In the update step, these prior states and their covariances are combined with the measurement to calculate the Kalman gain ( $\mathbf{K}_k$ ). Using the Kalman gain, the posterior states and their covariance are calculated:

$$\mathbf{K}_k = \hat{\mathbf{P}}_k^- \mathbf{C}_d^\top (\mathbf{C}_d \hat{\mathbf{P}}_k^- \mathbf{C}_d^\top + \mathbf{R})^{-1} \quad (5)$$

$$\hat{\mathbf{x}}_k = \hat{\mathbf{x}}_k^- + \mathbf{K}_k (\mathbf{y}_k - \mathbf{C}_d \hat{\mathbf{x}}_k^-) \quad (6)$$

$$\hat{\mathbf{P}}_k = (\mathbf{I} - \mathbf{K}_k \mathbf{C}_d) \hat{\mathbf{P}}_k^- \quad (7)$$

where  $\mathbf{I}$  is a unit identity matrix, and  $\hat{\mathbf{x}}_k$  and  $\hat{\mathbf{P}}_k$  are the estimate of posterior state and their covariance matrices, respectively. Because the Kalman filter is based on a Bayesian framework, which is a recursive process, the posterior states and their covariance are used as the prior time step states and covariance for the next step.

2) *Extended Kalman Filter*: Many practical system domain applications are non-linear resulting in the need for the EKF, which is applicable for both linear and non-linear systems [12]. Consider a discretized non-linear system and measurement model as below:

$$\mathbf{x}_k = \mathbf{f}_{k-1}(\mathbf{x}_{k-1}, \mathbf{u}_{k-1}) + \mathbf{w}_{k-1} \quad (8)$$

$$\mathbf{y}_k = \mathbf{h}_k(\mathbf{x}_k) + \mathbf{v}_k \quad (9)$$

where at discrete time  $k$ ,  $\mathbf{f}_k$  is the state function, and  $\mathbf{h}_k$  is measurement function. The steps for the EKF are similar to the KF, with the additional approximate linearization of the non-linear system around a nominal state trajectory for the estimation by computing the Jacobian matrices for the state and measurement,  $\mathbf{A}_{d(k-1)} \in \mathbb{R}^{n_x \times n_x}$  and  $\mathbf{C}_{d(k)} \in \mathbb{R}^{n_y \times n_x}$ , respectively:

$$\mathbf{A}_{d(k-1)} = \frac{\partial \mathbf{f}_{d(k-1)}}{\partial \mathbf{x}} \Bigg|_{\mathbf{x}_{k-1}, \mathbf{u}_{k-1}} \quad \text{and} \quad \mathbf{C}_{d(k)} = \frac{\partial \mathbf{h}_k}{\partial \mathbf{x}} \Bigg|_{\mathbf{x}_k} \quad (10)$$

The prediction step in (3)–(4) and the update step in (5)–(7) are then updated with  $\mathbf{A}_{d(k-1)}$  and  $\mathbf{C}_{d(k)}$  for  $\mathbf{A}_d$  and  $\mathbf{C}_d$ , respectively, to complete the EKF. As it is needed for the UKF in the next subsection, the state equation for EKF is provided below:

$$\hat{\mathbf{x}}_k^- = \mathbf{A}_{d(k-1)} \hat{\mathbf{x}}_{k-1} + \mathbf{B}_d \mathbf{u}_{k-1} \quad (11)$$

3) *Unscented Kalman Filter (UKF)*: EKF introduces a substantial error in the true posterior mean and covariance of the state transition and observation model, resulting in poor performance and, in certain cases, the filter diverging from the correct result [13]. UKF can be implemented in such a scenario, using a deterministic sampling approach called *unscented transformation* (UT) to address problems incorporated by EKF. Rather than taking the entire function, UKF conducts point-to-point transformation using sigma points, which are taken around the mean and propagated through the non-linear function by multiplying with certain weights. The transformed sigma points precisely capture the posterior mean and covariance to the third-order (Taylor series expansion) for

any non-linearity [13]. The accuracy of this technique depends on the weight assigned to each sigma point. So, an initial guess value of weight for each sigma point needs to be taken carefully before implementing UKF.

Let  $(\cdot)^{(i)}$  represent the  $i^{\text{th}}$  column of a matrix, and  $(\hat{\mathcal{X}}_{k-1}) \in \mathbb{R}^{n_x \times (2n_x+1)}$  represent the matrices of sigma points. Then generate  $2n_x+1$  sigma points from  $\hat{\mathbf{x}}_{k-1}$  as below [10], [13]:

$$\hat{\mathcal{X}}_{k-1}^{(i)} = \begin{cases} \hat{\mathbf{x}}_{k-1} & \text{for } i = 0 \\ \hat{\mathbf{x}}_{k-1} + \left( \sqrt{\alpha^2(n_x + \kappa)} \hat{\mathbf{P}}_{k-1}^{1/2} \right)^{(i)} & \text{for } i = 1, 2, \dots, n_x \\ \hat{\mathbf{x}}_{k-1} - \left( \sqrt{\alpha^2(n_x + \kappa)} \hat{\mathbf{P}}_{k-1}^{1/2} \right)^{(i-n_x)} & \text{for } i = n_x + 1, n_x + 2, \dots, 2n_x \end{cases}$$

where  $\alpha$  and  $\kappa$  are the parameters that determine the spread of sigma points around the mean value.

Now, transfer these sigma point through (11) to obtain modified sigma points  $\hat{\mathcal{X}}_k^- \in \mathbb{R}^{n_x \times (2n_x+1)}$  for estimating prior states and its covariance matrix as:

$$\hat{\mathcal{X}}_k^{(i)-} = \mathbf{f}_{k-1}(\hat{\mathcal{X}}_{k-1}^{(i)}), \quad \text{for } i = 0, 1, \dots, 2n_x \quad (12)$$

The prediction step from the prior KF type estimators is then replaced as:

$$\hat{\mathbf{x}}_k^- = \sum_{i=0}^{2n_x} w_m^{(i)} \hat{\mathcal{X}}_k^{(i)-} \quad (13)$$

$$\hat{\mathbf{P}}_k^- = \sum_{i=0}^{2n_x} w_c^{(i)} (\hat{\mathcal{X}}_k^{(i)-} - \hat{\mathbf{x}}_k^-) (\hat{\mathcal{X}}_k^{(i)-} - \hat{\mathbf{x}}_k^-)^\top + \mathbf{Q} \quad (14)$$

where

$$w_m^{(i)} = \begin{cases} 1 - \frac{n_x}{\alpha^2(n_x + \kappa)} & \text{for } i = 0 \\ \frac{1}{2\alpha^2(n_x + \kappa)} & \text{for } i = 1, 2, \dots, 2n_x \end{cases} \quad (15)$$

$$w_c^{(i)} = \begin{cases} (2 - \alpha^2 + \beta) - \frac{n_x}{\alpha^2(n_x + \kappa)} & \text{for } i = 0 \\ \frac{1}{2\alpha^2(n_x + \kappa)} & \text{for } i = 1, 2, \dots, 2n_x \end{cases} \quad (16)$$

In the above equations,  $\beta$  is the parameter to incorporate prior knowledge of the distribution of the state. For a Gaussian distribution,  $\beta=2$  is optimal, and  $w_m^{(i)}$  and  $w_c^{(i)}$  are the constant weights for calculation of mean and covariance, respectively [13].

Generate  $2n_x+1$  new sigma points  $\hat{\mathcal{X}}_k \in \mathbb{R}^{n_x \times (2n_x+1)}$  from  $\hat{\mathbf{x}}_k^-$  following the same procedure of generating sigma points as mentioned above. Propagate those sigma points through the measurement model below:

$$\hat{\mathcal{Y}}_k^{(i)} = \mathbf{h}_k(\hat{\mathcal{X}}_k^{(i)}) \quad \text{for } i = 0, 1, \dots, 2n_x \quad (17)$$

Compute prior mean  $(\hat{\mathbf{m}}_k^-) \in \mathbb{R}^{n_y}$  and prior covariance  $(\hat{\mathbf{S}}_k) \in \mathbb{R}^{n_y \times n_y}$  of the measurement, and then cross-

covariance of states and measurement ( $\hat{\mathbf{Z}}_k$ )  $\in \mathbb{R}^{n_x \times n_y}$  as below:

$$\hat{\mathbf{m}}_k^- = \sum_{i=0}^{2n_x} w_m^{(i)} \hat{\mathcal{Y}}_k^{(i)} \quad (18)$$

$$\hat{\mathbf{S}}_k = \sum_{i=0}^{2n_x} w_c^{(i)} (\hat{\mathcal{Y}}_k^{(i)} - \hat{\mathbf{m}}_k^-) (\hat{\mathcal{Y}}_k^{(i)} - \hat{\mathbf{m}}_k^-)^\top + \mathbf{R} \quad (19)$$

$$\hat{\mathbf{Z}}_k = \sum_{i=0}^{2n_x} w_c^{(i)} (\hat{\mathcal{X}}_k^{(i)} - \hat{\mathbf{x}}_k^-) (\hat{\mathcal{Y}}_k^{(i)} - \hat{\mathbf{m}}_k^-)^\top \quad (20)$$

The update step is replaced with:

$$\mathbf{K}_k = \hat{\mathbf{Z}}_k \hat{\mathbf{S}}_k^- \quad (21)$$

$$\hat{\mathbf{x}}_k = \hat{\mathbf{x}}_k^- + \mathbf{K}_k (\mathbf{y}_k - \hat{\mathbf{m}}_k^-) \quad (22)$$

$$\hat{\mathbf{P}}_k = \hat{\mathbf{P}}_k^- - \mathbf{K}_k \hat{\mathbf{S}}_k \mathbf{K}_k^\top \quad (23)$$

### C. Moving Horizon Estimation

UKF also can suffer from numerical instability [3], and KF, EKF, and UKF might fail in a system with non-Gaussian noise. MHE is introduced here, which can estimate both states and parameters at the current sampling time even in the presence of non-Gaussian measurement noise. MHE is an online optimization approach that leverages past measurement data over a finite horizon to estimate the states and parameters at the current time-step by minimizing a cost function while satisfying the constraints imposed on the states and parameters. The accuracy of MHE depends on the horizon window. If the horizon window is large then accuracy will, in general, be higher, but the computational cost increases, and vice-versa. There exists a trade-off in the accuracy and computation cost while implementing MHE, and can be implemented as per the underlying domain/control requirements. As MHE uses an iterative solver, an initial guess of states and parameters are required. Additionally, using domain knowledge, an appropriate range of parameter values should be imposed as constraints during estimation. States and parameters are estimated separately during estimation from MHE, unlike EKF/UKF. Let  $\Theta \in \mathbb{R}^{n_p}$  be the  $n_p$  parameters to be estimated. Now, considering a discretized non-linear system and measurement model as below:

$$\mathbf{x}_k = \mathbf{f}_{k-1}(\mathbf{x}_{k-1}, \mathbf{u}_{k-1}, \Theta) + \mathbf{w}_{k-1} \quad (24a)$$

$$\mathbf{y}_k = \mathbf{h}_k(\mathbf{x}_k, \Theta) + \mathbf{v}_k \quad (24b)$$

Let  $L$  be the backward length of window horizon,  $q$  be the discrete instant at present, and  $\mathcal{H}$  be the set of discrete time instants represented by  $\{q-L+1, q-L+2, \dots, q\}$ . The MHE can be formulated by two techniques: Bayesian updating of conditional probability, or minimization of defined cost function [14]. Although these two techniques are equivalent, as presented in [15], it is difficult to implement Bayesian updating of conditional probability techniques in MHE due to constraints on the estimation and non-linearity of the system. Therefore, minimization of a defined cost function is implemented, taking the following form:

$$\min_{\mathbf{x}_k, \Theta} J_L = \left( \left\| \mathbf{x}_L - \bar{\mathbf{x}}_L \right\|_{\mathbf{V}_L}^2 + \sum_{k=q-L+1}^q \left\| \mathbf{y}_k - \mathbf{h}(\mathbf{x}_k, \Theta) \right\|_{\mathbf{V}}^2 + \sum_{k=q-L+1}^{q-1} \left\| \mathbf{w}_k \right\|_{\mathbf{W}}^2 \right) \quad (25a)$$

subject to

$$\mathbf{x}_k = \mathbf{f}(\mathbf{x}_{k-1}, \mathbf{u}_{k-1}, \Theta) + \mathbf{w}_{k-1} \quad \forall k \in \mathcal{H} - \{q\} \quad (25b)$$

$$\Theta_{min} \leq \Theta \leq \Theta_{max} \quad (25c)$$

where  $\Theta_{min}$  and  $\Theta_{max}$  denotes the minimum and maximum possible values of parameters, respectively, and  $J_L$  represents the cost function to be minimized. In the cost function,  $\mathbf{x}_L$ ,  $\bar{\mathbf{x}}_L$ , and  $\bar{\Theta}_L$  represent the current states, previous estimated states, and previous estimated parameters at time  $k = q - L$ , respectively. Here, 1<sup>st</sup> term of (25a) represents the arrival cost which makes the use of previous instant estimated states, parameters, and their covariance matrix (similar to KF). Adding arrival cost gives a better estimate even with small horizon window and makes estimates at each sample instant better. This helps in achieving increasing certainty in states and parameter estimation at each sample instant, and thus, their weight also increases which implies that the weight of arrival cost at each sample-instant get changed. So, for updating weight, different methods are employed which can be found in the literature [16] [17]. Moreover,  $\mathbf{V}_L = \text{diag}(\mathbf{V}_0^x, \mathbf{V}_0^p)^{-1}$ , the diagonal matrix having state ( $\mathbf{V}_0^x$ ) and parameter covariance matrix ( $\mathbf{V}_0^p$ ),  $\mathbf{V} = \mathbf{R}^{-1}$  and  $\mathbf{W} = \mathbf{Q}^{-1}$ . Here, we adopt the notation from [15] where  $\|\mathbf{a}\|_{\mathbf{A}}^2 = \mathbf{a}^\top \mathbf{A} \mathbf{a}$  is the square of norm of vector  $\mathbf{a}$  with respect to matrix  $\mathbf{A}$ . Similarly, 2<sup>nd</sup> and 3<sup>rd</sup> term of (25a) are the residual of the process and measurement noise respectively. Equation (25b) represents the discretized model of the system, and (25c) represents parameter limits throughout the horizon window.

## III. PROCEDURE TO EVALUATE STATE AND PARAMETER ESTIMATORS

Each filter mentioned in the previous section was designed to estimate states, and parameters (except for KF). In this section, we model the frequency dynamics of a microgrid, including the states, i.e., change in rotor angle ( $\Delta\delta$ ), change in frequency ( $\Delta\omega$ ), and ROCOF ( $\Delta\dot{\omega}$ ), and parameters, i.e., damping constant ( $D$ ) and inertia constant ( $M$ ). The filtering method design criteria are applied to a simulation environment in Matlab/Simulink for estimator comparison. The incorporated system's frequency dynamic model, methods for comparing the performance of different filters, simulation setup, and parameter selection for design and implementation of the four filters are discussed in this section. The filters will be compared based on accuracy and computation time.

### A. Frequency Dynamics Model

The state-space representation of the linearized frequency dynamics of a power system [18] is given below:

$$\Delta\dot{\mathbf{x}} = \mathbf{A}\Delta\mathbf{x} + \mathbf{B}\Delta\mathbf{u} \quad (26)$$

where

$$\Delta \mathbf{x} = \begin{bmatrix} \Delta \delta \\ \Delta \omega \\ \Delta \dot{\omega} \end{bmatrix}, \quad \Delta \mathbf{u} = [\Delta P_e]$$

and,

$$\mathbf{A} = \begin{bmatrix} 0 & 1 & 0 \\ 0 & 0 & 1 \\ -\frac{K_i}{MT_g} & -\left(\frac{D}{MT_g} + \frac{1}{R_p MT_g}\right) & -\left(\frac{D}{M} + \frac{1}{T_g}\right) \end{bmatrix}$$

$$\mathbf{B} = \begin{bmatrix} 0 \\ 0 \\ -\frac{1}{MT_g} \end{bmatrix}$$

where,  $R_p$ ,  $T_g$ ,  $\Delta P_e$  and  $K_i$  are the speed-regulation droop constant, time constant of turbine governor, change in electrical power, and secondary control loop integral gain respectively.

### B. Methods for Performance Comparison

The filters will be compared based on accuracy and computation time. The system state is time-varying in nature. To compute the filter error, the maximum and minimum values of the states at a given time instant should be considered. For this study, we use the normalized root mean square error (NRMSE) to calculate the error, given as:

$$\text{NRMSE} = \left( \frac{\|\hat{y}(t) - y(t)\|_2}{\sqrt{N} (\max(\hat{y}(t)) - \min(\hat{y}(t)))} \right) \times 100\%$$

where,  $\|\cdot\|_2$  represents Euclidean norm,  $y(t)$  is the actual value of states,  $\hat{y}(t)$  is the estimated value of states and  $N$  is the number of data point considered.

Because the parameters are (assumed) constant and time-independent, the root mean square error (RMSE) is used to calculate parameter estimation error, given as:

$$\text{RMSE} = \left( \frac{\|y(t) - \text{mean}(\hat{y}(t))\|_2}{\sqrt{N} (\text{mean}(\hat{y}(t)))} \right) \times 100\%$$

Note that although we are not changing the parameters through time in this study, the MHE has been shown to track these time-varying changes in [18]. Each of the filters is also monitored for computation time, reported as the average time the filtering step takes per time-step of the simulation.

### C. Simulation Setup, Parameters Selection and Filter Implementation

The simulation setup to carry out the state and parameter estimation of the above system frequency dynamics model using different filters is shown in Fig. 1. The power system model and each of the filters was developed in Matlab/Simulink and simulated on an Opal-RT real-time simulator located at South Dakota State University. The simulation parameters are listed

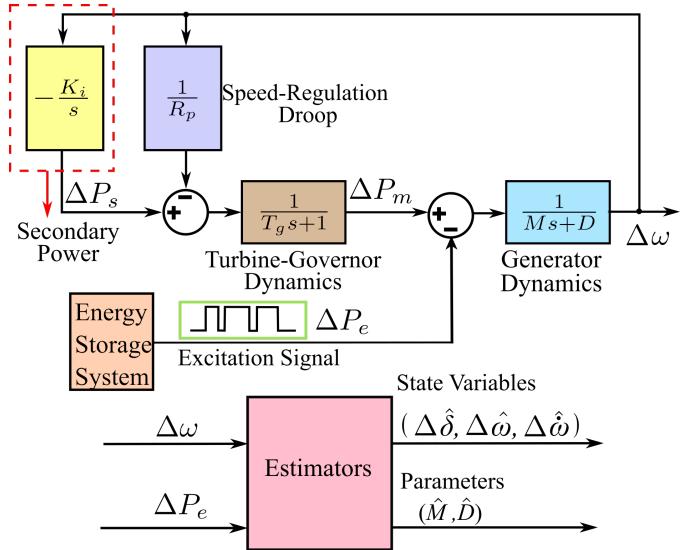


Fig. 1. Simulation setup for state and parameter estimation using different estimation filters. This model was setup in Matlab/Simulink and deployed on an Opal-RT real-time simulator.

TABLE I  
SUMMARY OF SIMULATION PARAMETERS

Parameter	Values
Inertia Constant (M)	4s
Damping Coefficient (D)	1.50%
Speed Regulation Droop ( $R_p$ )	5%
Turbine-Governor Time Constant ( $T_g$ )	0.2s
Integral Gain ( $K_i$ )	2.0
Sample time ( $T_s$ )	0.02s

in Table I. The time constant ( $\tau$ ) of the frequency dynamics model represented by (26) is given as [19]:

$$\tau = \frac{2MT_g}{M + DT_g} \quad (27)$$

In (27),  $M$ ,  $D$  and  $T_g$  are assumed values that can be noted from Table I; ( $T_s$ ) is then chosen to be 20 times smaller than the value of the time constant (as described in Section II-A), and hence a 0.02 s sample time is obtained.

As  $\Delta\omega$  can be measured from a Phase Locked Loop (PLL), it is considered a measurable state variable. Additionally,  $\Delta\omega$  is sufficient to make the correct estimation of other states and parameters; this insight was obtained by performing an observability analysis of the system [14].

To check the performance of filters under noisy condition, random noise ( $v_k$ ) was added to the measured  $\Delta\omega$  signal which resulted in a signal-to-noise ratio (SNR) of 55 dB [18]. Thus, the measurement noise covariance  $\mathbf{R}$  is designed assuming the SNR is known ( $\text{SNR}_{\text{dB}} = 20 \log \left( \frac{1}{\sigma} \right)$  [20] from which  $\mathbf{R} = \sigma^2$ ), which would correspond to a covariance of  $\approx 10^{-6}$ . Additionally, the process noise covariance matrix  $\mathbf{Q} = \text{diag}(Q_{\Delta\delta}, Q_{\Delta\omega}, Q_{\Delta\dot{\omega}}, Q_D, Q_M)$  associated with the states and parameters  $[\Delta\delta, \Delta\omega, \Delta\dot{\omega}, D, M]$  was designed as follows: because the expected process noise can be considered relatively small compared to the measurement noise,  $Q_{\Delta\omega}$

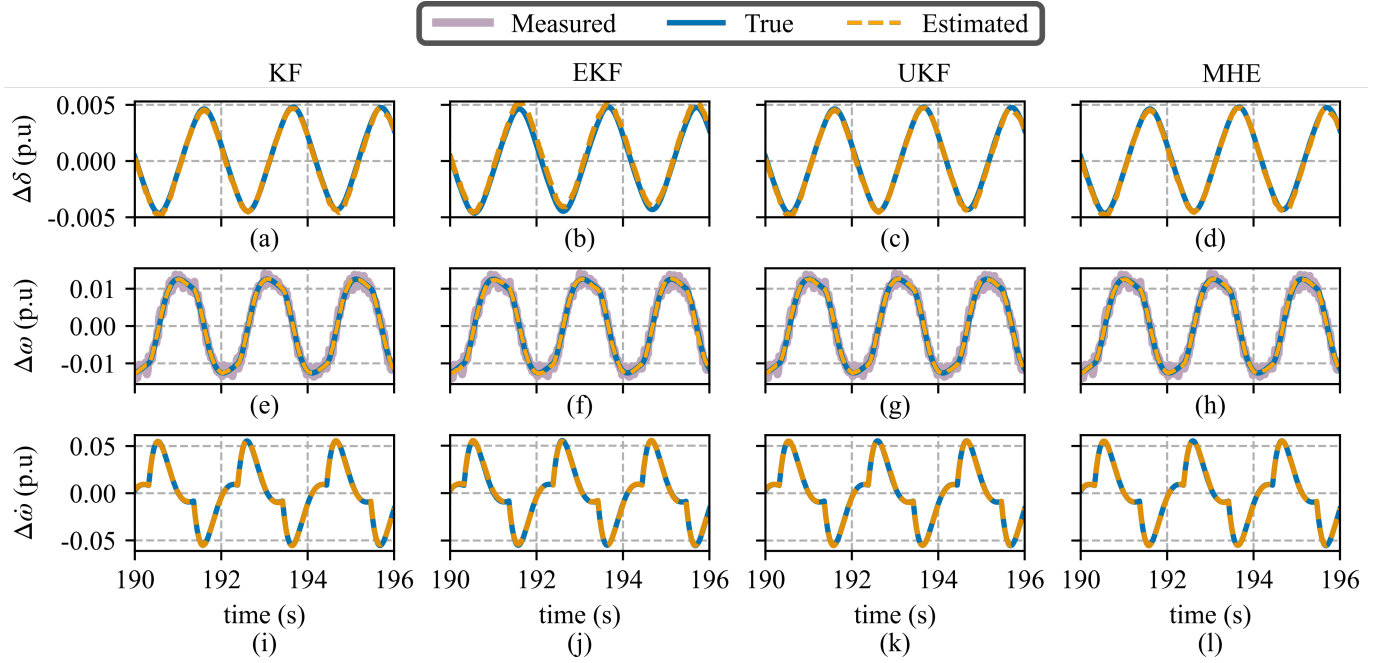


Fig. 2. Estimation of states using different filters. First (a-d), second (e-h) and third row (i-l) represent estimation  $\Delta\delta$ ,  $\Delta\omega$ ,  $\Delta\dot{\omega}$  respectively. First, second, third and fourth column are for KF, EKF, UKF and MHE respectively. Note:  $\Delta\omega$  is the only measured state (shaded gray envelope).

was assumed to be 100 times smaller than  $\mathbf{R}$ . The other terms were obtained by multiplying  $Q_{\Delta\omega}$  to the respective state and parameter sensitivity to variations on  $\Delta\omega$ . Thus,  $\mathbf{Q} = \text{diag}(0.5 \times 10^{-8}, 10^{-8}, 5 \times 10^{-8}, 10^{-4}, 10^{-3})$ .

For the MHE implementation, the horizon length of MHE chosen followed the rule of thumb of twice the order of the system [16]. Since we are estimating three states ( $\Delta\delta$ ,  $\Delta\omega$ , and  $\Delta\dot{\omega}$ ) and two parameter ( $D$  and  $M$ ) (5<sup>th</sup> order system), the horizon length taken was 10. The weights for MHE ( $\mathbf{V}$  and  $\mathbf{W}$ ) were chosen as the  $\mathbf{R}^{-1}$  and  $\mathbf{Q}^{-1}$ , respectively [15]. In addition, an EKF based on deterministic sampling was used to update the arrival cost function of MHE.

To perturb the system, three different types of excitation signals were used and analyzed, emulating an ESS actively exciting the system to estimate parameters and states. First, a square wave in the form of a pulse train having an amplitude of 0.2 p.u. and frequency 0.5 Hz was used. Next, a chirp signal having an amplitude of 0.2 p.u. and frequency ranging from 0.1 Hz to 0.5 Hz was used. The selected frequency range lies in the frequency band of interest corresponding to the normal inertia constant range [21], [22]. Finally, a square chirp signal having the same amplitude and frequency range as that of a chirp signal was used. The error in estimation was found to be minimum with square chirp signal, so that signal was considered as the excitation signal for making comparative analysis of different filters in all results.

Using the measured noisy  $\Delta\omega$  and square chirp signal as an input to the different filters, state and parameter estimation of the simplified frequency dynamic model was conducted. Because KF can only estimate the states of a linear system, the parameters  $M$  and  $D$  are considered as known constants, and only states  $\Delta\delta$ ,  $\Delta\omega$ , and  $\Delta\dot{\omega}$  were estimated. The initial

condition for all states were selected as (0, 0, 0), because using domain knowledge the change in all the states was expected to be ideally zero. During the implementation of EKF and UKF,  $D$  and  $M$  were incorporated as state variables and their derivatives were set to zero and estimated along with ( $\Delta\delta$ ,  $\Delta\omega$  and  $\Delta\dot{\omega}$ ). For these two filters, the initial condition for states and parameters were taken as (0, 0, 0, 2, 2) following the order of  $\Delta\delta$ ,  $\Delta\omega$ ,  $\Delta\dot{\omega}$ ,  $M$ , and  $D$ . In the case of MHE, the states and parameters were estimated separately by using a CasADi open-source tool. For MHE, the initial guess values were also taken as (0, 0, 0, 2, 2) following the same order as in EKF and UKF. The four filters were implemented in the OP5707 Opal-RT real-time digital simulator, with specifications shown in Table II. After developing the model in MATLAB/Simulink, the model was divided into three different subsystems (i.e., master, slave, console) in RT-lab. The master subsystem contains the frequency dynamics of the system, the slave contains the filters, and the measurements were visually observed in the console subsystem. For the MHE implementation in the real-time simulator, *qrqp* solver was used in our experiment. First, the optimization problem was formulated using CasADi, and a solver instance was created. C code was generated for the solver instance which was interfaced to Simulink via the S-function builder. In RT-Lab, the generated C code was added (which will be compiled by RT-Lab). After implementing in RT-Lab, the model was run in OP5707. The files that are necessary to run the S-function (CasADi generated code, interface code and S-function generated wrapper files) should be uploaded in the file properties. Then the model was built, loaded, and executed. The simulation was carried out for 200 s for each of the filters, which was a sufficient time frame for making a comparative analysis as each of the estimators

converged around a steady-state value.<sup>1</sup>

TABLE II  
SPECIFICATION OF OP5707 REAL-TIME SIMULATOR.

Item	Description
Processor	Intel® Xeon® CPU E5-2698 v3 (i686) @2.30GHz
Operating System	Red Hat Enterprise Linux Server release 5.2(Tikanga)
Compiler	opicc/opicpc 11.1
Cache size	40.96MB
Activated core for real-time simulation	6

#### IV. RESULTS AND ANALYSIS

The estimation of  $\Delta\delta$ ,  $\Delta\omega$ ,  $\Delta\dot{\omega}$ , under the influence of Gaussian noise, using different filters are presented in Figs. 2(a-d), Figs. 2(e-h), and Figs. 2 (i-l), respectively (i.e., each row). Each column of Fig. 2 shows the results of one of the filters. All states estimated approximately track the true states for all filters.

The NRMSE between the estimated states and the true states for the different filters is listed in Table III. The NRMSE in  $\Delta\delta$  is consistently higher for all filters compared with  $\Delta\omega$  and  $\Delta\dot{\omega}$ . This can be attributed to the design of the  $Q$  and  $R$  matrices, that could be further adjusted to prioritize the state estimation (model fit) to minimize the error of a certain state/parameter as compared to others.

TABLE III  
COMPARISON OF NRMSE, RMSE AND COMPUTATION TIME OF KF, EKF, UKF AND MHE

Filters	NRMSE (%)			Computational Time ( $\mu s$ )		RMSE (%)	
	$\Delta\delta$	$\Delta\omega$	$\Delta\dot{\omega}$	$D$	$M$	$D$	$M$
KF	6.152	3.247	2.019	0.95	-	-	-
EKF	6.326	4.054	1.968	1.22	3.031	0.319	-
UKF	5.930	3.863	1.871	1.94	2.945	0.318	-
MHE	5.689	3.972	1.881	209.52	2.913	0.320	-

The estimated  $M$  and  $D$  parameters while using EKF, UKF and MHE are depicted as a probability density plot in Fig. 3 taken as the kernel density estimate of the discrete-time estimates. Each of the three filters estimated the parameters accurately, with the mean approximately the true value. However, the accuracy of estimation varies slightly depending on the type of filter. It can also be noted from Table III that error in  $D$  is comparatively higher as compared to  $M$  for every filter because  $D$  does not have a significant influence on the frequency dynamics; the estimation of  $D$  while considering a frequency dynamics system will have greater uncertainty [14].

The computation time required for each of the different filters is listed in Table III. The function “clock\_gettime()” of “time.h” header file is used to compute the time required to execute each filter for one time step. MHE required comparatively higher computation time for estimation compared to the

<sup>1</sup>The code and models to run the state estimation framework are available as open source at: [https://github.com/TaraAryal/All\\_Estimation\\_Filters/tree/Filters\\_Design\\_Simulink](https://github.com/TaraAryal/All_Estimation_Filters/tree/Filters_Design_Simulink).

single-step recursive filters, however, it is fast enough for real-time state and parameter estimation of power system frequency dynamics. It has been noted that each filter yields a reasonable state and parameter (sans KF) estimation. However, it is important to report that the initial guess value of parameters played an important role in the convergence of EKF. The EKF filters diverged when the initial guess value of  $D$  and  $M$  were taken far from the true value (e.g., 0.1 and 0.1) from its true value (1.5, 4), but the filters provided accurate estimates when initial guess (2, 2) was closer to their true value. Additionally, the method of updating the weights of sigma points plays an important role in numerical stability of UKF. Based on the underlying system, if a correct method is not chosen to update weights, then UKF may have instability issues depending on initial guess values. In contrast, MHE estimates the states and parameters without depending on initial guess values of parameters.

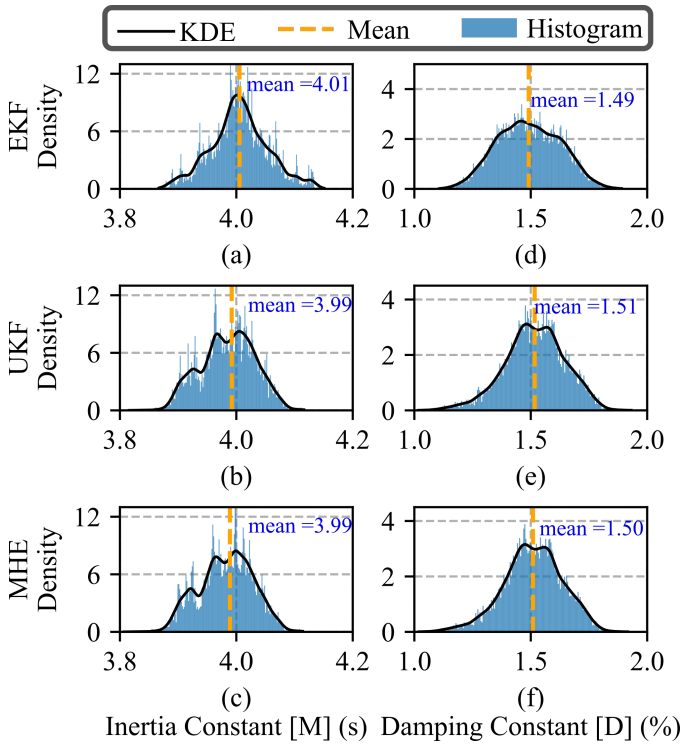


Fig. 3. Estimation of parameters using different filters. First (a-c) and second (d-f) column represents estimation of inertia and damping constant respectively. First, second and third row are for EKF, UKF, MHE respectively.

#### A. Discussion on Non-Gaussian Noise

The distribution of  $v_k$  is time-variant and deteriorates with the current transformers, potential transformers, and change in communication channels implemented in the system [23]. Thus, non-Gaussian noise was also incorporated to compare the filter performance. The skewness and kurtosis metrics were used to characterize the noise deviation from a Gaussian distribution. Simulation was carried out for non-Gaussian noise with mean = 0,  $\mathbf{R} = 10^{-6}$  (same as Gaussian noise), and kurtosis = 7 [18] at different values of skewness starting

from 0 to 2.4. When the skewness was increased above this value, there is no distribution that could produce a non-Gaussian distribution that met the specified mean, covariance, and kurtosis. Due to space limitations, a rigorous study on estimation of states and parameters from different filters under different non-Gaussian noise conditions is left for future work. However, the results shows that KF family, while no longer provably optimal, still performed as similar as MHE under the non-Gaussian noise conditions studied. Furthermore, there were several skewness values (i.e., 1, 1.5, 1.75) where UKF failed to estimate; the cause for this is thought to be due to UKF's inherent instability. Our initial analysis was non-exhaustive, and conclusive statements about the KF family versus MHE under non-Gaussian noise cannot yet be made for power system frequency dynamics. Because the non-Gaussian noise covariance can be considered quite small, our initial results did not follow what has typically been reported in the literature (e.g., [24]).

## V. CONCLUSIONS

This paper compared four different power system frequency dynamics state and parameter estimation methods. All filters provided acceptable estimates in terms of accuracy for states, and EKF, UKF and MHE also properly estimated parameters. EKF presented convergence issues depending on the initial guess of parameters, whereas UKF faced numerical instability at certain initial guesses. MHE neither showed such convergence issues nor numerical instability due to initial guess during estimation, but required higher computation time, however, it is fast enough for real-time applications. Thus, if only states of the system are to be estimated then, KF can be employed. Similarly, if the expected value of parameters are within a narrow range, EKF and UKF might be satisfactorily employed for state/parameter estimation for fast frequency response. If the computation time of MHE is fast enough for the domain application, it can be considered a better option as it does not suffer from convergence issues due to initial guesses. The preliminary comparative analysis under certain non-Gaussian noise with small covariance showed KF family performed as similar as MHE. However, there was not enough evidence to support the results to fully conclude under those overall noise characteristics. The effect of non-Gaussian noise with large covariance or multi-modes was not evaluated and is part of our future work.

## ACKNOWLEDGMENTS

The authors would like to thank Dr. Alvaro Furlani Bastos from Sandia National Laboratories for the technical review of this paper.

## REFERENCES

- [1] J. Zhao, M. Netto, Z. Huang, S. S. Yu, A. Gómez-Expósito, S. Wang, I. Kamwa, S. Akhlaghi, L. Mili, V. Terzija, A. P. S. Meliopoulos, B. Pal, A. K. Singh, A. Abur, T. Bi, and A. Rouhani, "Roles of dynamic state estimation in power system modeling, monitoring and operation," *IEEE Transactions on Power Systems*, vol. 36, no. 3, pp. 2462–2472, 2021.
- [2] U. Tamrakar, D. A. Copp, T. Nguyen, T. M. Hansen, and R. Tonkoski, "Optimization-based fast-frequency estimation and control of low-inertia microgrids," *IEEE Transactions on Energy Conversion*, vol. 36, no. 2, pp. 1459–1468, 2021.
- [3] A. Sharma and S. K. Jain, "A review and performance comparison of power system state estimation techniques," in *2018 IEEE Innovative Smart Grid Technologies - Asia (ISGT Asia)*, 2018, pp. 770–775.
- [4] A. Khandelwal and A. Tondan, "Power system state estimation comparison of Kalman filters with a new approach," in *2016 7th India International Conference on Power Electronics (IICPE)*, 2016, pp. 1–6.
- [5] N. Zhou, D. Meng, Z. Huang, and G. Welch, "Dynamic state estimation of a synchronous machine using PMU data: A comparative study," *IEEE Transactions on Smart Grid*, vol. 6, no. 1, pp. 450–460, 2015.
- [6] G. A. Perdikaris, *Discrete-Time Systems*. Dordrecht: Springer Netherlands, 1991, pp. 139–234.
- [7] B. J. Odelson, M. R. Rajamani, and J. B. Rawlings, "A new autocovariance least-squares method for estimating noise covariances," *Automatica*, vol. 42, no. 2, pp. 303–308, 2006.
- [8] Z. Zheng, Y. Xu, L. Mili, Z. Liu, M. Korkali, and Y. Wang, "Observability analysis of a power system stochastic dynamic model using a derivative-free approach," *IEEE Transactions on Power Systems*, vol. 36, no. 6, pp. 5834–5845, 2021.
- [9] J. Pierre, N. Zhou, F. Tuffner, J. Hauer, D. Trudnowski, and W. Mittelestadt, "Probing signal design for power system identification," *Power Systems, IEEE Transactions on*, vol. 25, pp. 835 – 843, 06 2010.
- [10] D. Simon, *Optimal State Estimation: Kalman, H infinity and nonlinear approaches*. Wiley-Interscience, 2006.
- [11] G. Welch and G. Bishop, *An Introduction to the Kalman Filter*. University of North Carolina at Chapel Hill, 1995.
- [12] Q. Li, R. Li, K. Ji, and W. Dai, "Kalman filter and its application," in *2015 8th International Conference on Intelligent Networks and Intelligent Systems (ICINIS)*, 2015, pp. 74–77.
- [13] E. Wan and R. Van Der Merwe, "The unscented Kalman filter for nonlinear estimation," in *Proceedings of the IEEE 2000 Adaptive Systems for Signal Processing, Communications, and Control Symposium (Cat. No.00EX373)*, 2000, pp. 153–158.
- [14] N. Bhujel, T. M. Hansen, R. Tonkoski, U. Tamrakar, and R. H. Byrne, "Optimization-based estimation of microgrid equivalent parameters for voltage and frequency dynamics," in *IEEE Madrid PowerTech*, 2021, pp. 1–6.
- [15] J. B. Rawlings, D. Q. Mayne, and M. Diehl, *Model predictive control: Theory, computation, and design*. Nob Hill Publishing, 2020.
- [16] C. V. Rao and J. B. Rawlings, "Constrained process monitoring: Moving-horizon approach," *American Institute of Chemical Engineers. AIChE Journal*, vol. 48, no. 1, p. 97, Jan 2002.
- [17] S. Ungarala, "Computing arrival cost parameters in moving horizon estimation using sampling based filters," *Journal of Process Control*, vol. 19, no. 9, pp. 1576–1588, 2009.
- [18] U. Tamrakar, D. A. Copp, T. A. Nguyen, T. M. Hansen, and R. Tonkoski, "Real-time estimation of microgrid inertia and damping constant," *IEEE Access*, vol. 9, pp. 114 523–114 534, 2021.
- [19] N. Bhujel, T. M. Hansen, R. Tonkoski, U. Tamrakar, and R. H. Byrne, "Model predictive integrated voltage and frequency support in microgrids," in *52nd North American Power Symposium (NAPS)*, 2021, pp. 1–6.
- [20] M. Brown, M. Biswal, S. Brahma, S. J. Ranade, and H. Cao, "Characterizing and quantifying noise in pmu data," in *IEEE Power and Energy Society General Meeting (PESGM)*, 2016, pp. 1–5.
- [21] P. Kundur, *Power System Stability and control*. McGraw Hill, 1994.
- [22] M. Rauniyar, S. Berg, S. Subedi, T. M. Hansen, R. Fournier, R. Tonkoski, and U. Tamrakar, "Evaluation of probing signals for implementing moving horizon inertia estimation in microgrids," in *52nd North American Power Symposium (NAPS)*, 2021, pp. 1–6.
- [23] S. Wang, J. Zhao, Z. Huang, and R. Diao, "Assessing Gaussian assumption of PMU measurement error using field data," *IEEE Transactions on Power Delivery*, vol. 33, no. 6, pp. 3233–3236, 2018.
- [24] X. Sun, J. Duan, X. Li, and X. Wang, "State estimation under non-Gaussian Lévy noise: A modified Kalman filtering method," *arXiv preprint arXiv:1303.2395*, 2013.